THE ASTROPHYSICAL JOURNAL, 247:869–878, 1981 August 1

ABUNDANCES IN GLOBULAR CLUSTER RED GIANTS. IV. M22 AND OMEGA CENTAURI

JUDITH G. COHEN[1]
Palomar Observatory, California Institute of Technology; and Kitt Peak National Observatory[2]
Received 1980 October 27; accepted 1981 January 16

ABSTRACT

A detailed abundance analysis has been performed for three members of M22 and five of ω Cen. The three giants in M22 are chemically identical with [Fe/H] = −1.78 dex except for a range of Na and, less certainly, Ba larger than the observational and modeling errors. The ω Cen giants show a range of abundance for all elements, with the light elements and the rare earths (plus Ba) enhanced by a larger factor than the Fe peak nuclei in the more metal-rich ω Cen stars. The two most metal-rich ω Cen stars have vastly different Na/Mg and Al/Mg ratios and Sc abundances. Explosive nucleosynthesis fails to predict the Na/Mg observed ratios at large Al/Mg values. The deduced neutron excesses are $\eta \approx 10^{-2}$ and 5×10^{-4}; the former is the largest known for any star. These high values of η require massive ($M \geq 12\ M_{\odot}$) supernova progenitors and may also produce via the *s*-process the strong enhancement of Ba and the rare earths seen in the metal-rich ω Cen giants. It is suggested that such massive supernovae were much rarer in the less dense halo field, leading to the observed differences in abundance patterns of globular cluster giants versus halo field dwarfs.

Subject headings: clusters: globular — nucleosynthesis — stars: abundances — stars: supernovae

I. INTRODUCTION

In this series of papers we attempt to provide fundamental determinations of the abundances of chemical elements in globular cluster red giants. In the first three papers of this series, members of globular clusters of low (Cohen 1979), intermediate (Cohen 1978*a*, hereafter Paper I), and high (Cohen 1980*a*, hereafter Paper III) metallicity were analyzed. In this work we discuss three members of M22 and five members of ω Cen. The latter cluster is clearly anomalous; it has long been realized that the giant branch of ω Cen is considerably wider in $B-V$ than that of any other globular cluster (Woolley *et al.* 1966; Dickens and Woolley 1966; Cannon and Stobie 1973). Strong evidence has been found for a spread of at least one order of magnitude in heavy metal abundance among the RR Lyrae variables (Butler, Dickens, and Epps 1978) and among the giants (Norris 1978; Cohen 1978*b*; Lloyd Evans 1978) in this unique cluster. M22 was for a long time believed to be a less extreme example than ω Cen of the above phenomena (Hesser, Hartwick, and McClure 1977). However, recent work by Lloyd Evans (1978) has shown that most, if not all, of the evidence for a range in heavy element abundances within M22 is due to inadequate membership studies and confusion by field stars, although evidence for a range in CN strengths still exists (Hesser and Harris 1979).

The observational material and model atmosphere parameters for the ω Cen and M22 giants are described in § II, while the deduced abundances are detailed in § III. In the next section we describe the range of abundances of the various elements found in ω Cen. The results are summarized in § V, and in the Appendix we give information on the interstellar lines and Hα emission found in these globular cluster giants. A preliminary account of this work was given by Cohen (1980*b*).

II. OBSERVATIONAL MATERIAL

Three of the bright giants (II-31, IV-20, and IV-59) in M22 with photometry by Eggen (1977) or Lloyd Evans (1975) were chosen as program stars. Two of the three were included in an unpublished program of infrared photometry of 19 stars in M22 by Frogel and Cohen, from which effective temperatures and surface gravities (assuming a mass of 0.8 $M_{\odot}$) were obtained as described in Cohen, Frogel, and Persson (1978). $E(B-V) = 0.36$ mag was used, which is a mean of that determined by Harris and Racine (1979) and by Zinn (1980) and is close to that found for early-type foreground stars by Hesser (1976), together with Zinn's distance modulus. The remaining star, IV-59, was too crowded for infrared photometry, and its $T_{\rm eff}$ was determined from its visual magnitude and the shape of the giant branch in the H-R diagram deduced from the infrared sample. As indicated in the Appendix, all three stars are radial velocity members of M22.

Persson *et al.* (1980, henceforth PFCAM) have presented infrared photometry for 82 stars on the upper giant branch of ω Cen. Five stars were chosen (ROA 213, 58, 102, 253, and 219) from their sample which were bright, had $4000 \leq T_{\rm eff} \leq 4500$ K, and spanned the wide giant branch. The values of $T_{\rm eff}$ and log g for these stars were taken directly from Table 2 of PFCAM, and are listed in Table 1, together with the appropriate data for the M22

[1] Visiting Astronomer, Cerro Tololo Inter-American Observatory.
[2] Operated by the Association for Research in Astronomy, Inc., under contract with the National Science Foundation.

TABLE 1

MODEL ATMOSPHERE PARAMETERS

Star	$T_{\rm eff}$	log (g)[a]	$Z/Z_\odot$	V_t (km s^{-1})	$R(V-K)$[b]
M22:					
II-31	4350	1.0	0.03	2	...
IV-20	4300	1.1	0.03	2	...
IV-59	4300	1.1	0.03	2	...
ω Cen:					
213	4500	1.1	0.01	2	0.06
58	4200	0.6	0.01	2.5[c]	0.13
102	4200	0.7	0.01	3[c]	0.16
253	4300	1.0	0.03	2	0.25
219	4000	0.7	0.03	2	0.42

[a] A stellar mass of 0.8 $M_\odot$ is always assumed.
[b] $R(V-K)$ is a metallicity parameter whose values are taken from PFCAM.
[c] V_t changed to 2 km s^{-1} in the final analysis.

program stars. In addition, PFCAM's metallicity parameter $R(V-K)$, determined from broad-band photometry via the location of a star in the H-R diagram and defined to be 0.0 at the metallicity of M92 and 0.71 at the metallicity of M71, is listed in Table 1 for the ω Cen stars. All five giants are, as shown in the Appendix, radial velocity members of this globular cluster. As an initial guess, an abundance of $\frac{1}{30}$ that of the Sun was adopted for M22 based on its color-magnitude diagram, and initial abundance parameters were assigned to the ω Cen giants based on their metallicity parameters $R(V-K)$ and the results of previous papers in this series for M92 and M71.

All observations were made during the inaugural testing phase of the CTIO 4 m echelle spectrograph in 1978 May with the Singer camera, the 226-1 cross disperser centered at 5500 Å, and baked IIIa-J plates. At that time, only the 31.6 groove mm^{-1} echelle was available, which gives approximately the same dispersion as the 79 groove mm^{-1} echelle used previously, but the orders are closer together, so that less widening is possible and no comparison spectrum can be used. Because of its smaller free spectral range, this echelle also provides more complete wavelength coverage than does the 79 groove mm^{-1}. Two good quality spectra were taken for each star as listed in Table 2; sensitometer plates were taken with each exposure and developed simultaneously with the spectra.

The spectra were traced with the PDS digital microphotometer by Mr. Ed. Carder of KPNO, converted to intensity, and the lines were identified by using the same procedures and computer software described in Paper I. The basic list of lines measured was that of Paper III, but due to the small spacing between echelle orders, which becomes smaller at shorter wavelengths, equivalent widths were not measured for $\lambda < 5400$ Å. The line list was amended to include suitable unblended features in those wavelength regions which fell between the echelle orders in the earlier specta. This additional wavelength coverage between 6700 and 5400 Å provided new lines for those elements with only a few lines in Paper III. For example, previously only the Na D doublet was accessible, while with the 31.6 groove mm^{-1} echelle, six Na I features were available.

Equivalent widths were determined from all the spectra and weighted as described in Paper I (the weights for each spectrum are listed in Table 2). One plate for each star

TABLE 2

PLATE JOURNAL

	Spectrum 1			Spectrum 2		
Star	Number[a]	t (minutes)	Weight	Number[a]	t (minutes)	Weight
M22:						
II-31	55	61	5	62	76	3
IV-20	63	61	5	56	60	3
IV-59	57	60	4	64	60	4
ω Cen:						
213	61	76	3	66	61	4
58	50	30	4	51	40	4
102	52	53	4	58	60	3
253	67	75	5	68	77	5
219	53	60	4	59	72	5

[a] All spectra are in the CTIO G series.

TABLE 3

MEASURED EQUIVALENT WIDTHS

	Line	EP	log gf	V_t (hfs)	log C_6	M22 II-31	M22 IV-20	M22 IV-59	ω Cen 213	ω Cen 58	ω Cen 102	ω Cen 253	ω Cen 219
OI	6363.8	0.02	-10.30			≤20	≤20	≤15		≤15			≤38
	6300.3	0.00	-10.00			≤20	≤24	≤17	≤22	29:	45	≤25	71:
NaI	6160.7	2.10	- 1.27			≤15	38			22:	33:	42	59
	6154.2	2.10	- 1.57			≤16	≤10	31		18:		43:	28:
	5895.9	0.00	- 0.19		-30.9	234	384	398	201	347	350	396	425
	5889.9	0.00	+ 0.11		-30.9	319	472	448	246	432	402	464	484
	5688.2	2.10	- 0.40			33:			61	73	95:	172	115
	5682.6	2.10	- 0.71			13:			40	45	56:	125	103
MgI	5711.1	4.34	- 1.58			70:			42	79	60	51	116
	5528.4	4.34	- 0.48		-30.5	219:					167:		295:
AlI	6698.7	3.14	- 1.73									76	50:
	6696.0	3.14	- 1.43									79	56:
SiI	6145.0	5.61	- 1.52			23:	21:		12:			29:	26
	5948.6	5.08	- 1.14			38	51	51	30	35	36	80	74
	5690.4	4.93	- 1.87			14:				8:	15:	36	25
CaI	6572.8	0.00	- 4.31		-31.2	62	89	59		94			186:
	6499.6	2.52	- 1.04		-30.5	101	89	80		64			103:
	6493.8	2.52	- 0.43		-30.5	113	145	106		134			121:
	6471.7	2.52	- 0.90		-30.5	82	107	84		73:			143:
	6439.1	2.53	- 0.08		-30.5	121	127	110		136			173:
	6169.5	2.53	- 0.72		-29.7	113	118	81	80	120	84:	124	
	6169.0	2.52	- 0.93		-29.7	74	82	54	44	81	93:	102	
	6166.4	2.54	- 1.30		-29.7	41	50	49	60	54	45:	73	108:
	6162.2	1.90	- 0.25		-30.0	155	168	152	133	184	172	392	209:
	6161.3	2.52	- 1.31		-29.7	29	38	42	21	38	34	42	72:
	6122.2	1.89	- 0.43		-30.0	152	148	173	142	178	184	212	288
	5867.6	2.93	- 1.41		-30.7			20	9	20	17	24	72
	5857.5	2.93	+ 0.17		-30.7	128	149	127	103	140	126	158	225
	5601.3	2.53	- 0.69		-30.4	71:			48:	63	62:		142
	5590.1	2.52	- 0.66		-30.4	101:			55:	89	69:		127
	5588.8	2.53	+ 0.14		-30.4	156:			110:	106	111:		161
	5582.0	2.52	- 0.54		-30.4	74:			56:	68	104:		164
ScI	5671.8	1.45	+ 0.39	2.8					18	15	35:	68	77
ScII	6604.6	1.36	- 1.33			48	61						
	5669.0	1.50	- 1.17			66:			44	69	57:	111	112
	5641.0	1.50	- 1.05			58:			56:	91	70:		76
	5526.8	1.77	- 0.07			106:					120:		
TiI	6556.1	1.46	- 0.85			22	44	42		39:			122:
	6554.2	1.44	- 0.90			33:	49	23		34			142:
	6419.1	2.17	- 1.12										33:
	6336.1	1.44	- 1.07			25:	24	22:					88:
	6126.2	1.07	- 0.96			48	61	52	15	38	46	56	146
	6121.0	1.88	- 0.84			22		35	8:	11:	16	22	64
	6091.2	2.27	+ 0.02								13:	20	10:	21	66
	6064.6	1.05	- 1.50				52	35:			36	34	23	49	113
	6031.7	0.05	- 3.37								16	13	20	45	66
	5978.6	1.87	- 0.16			29	31	43:			13	73	40	56	122
	5965.8	1.88	- 0.08			35	60				18	36	60	62	118
	5944.7	0.00	- 3.42			21:	31	37			14		23	13:	71
	5941.8	1.05	- 1.06			22	45	27			26	40	55	58	110
	5940.7	0.05	- 2.70				22:	21			14		14:	24	81
	5937.8	1.07	- 1.47			24	47:	27			19		34	36	126
	5922.1	1.05	- 1.06			33	66	57			28	76	48	100	165
	5918.6	1.07	- 1.14			30	38				17	52	42	52	114
	5903.3	1.07	- 1.58			77:	31	34:			23:	25	27	20	77
	5899.3	1.05	- 0.83								42	76	68	74	153
	5866.5	1.07	- 0.52			87	104	84			52	136	124	111	196
	5823.7	2.27	- 0.50								13:	31	14	30	36
	5689.5	2.30	- 0.04								14		17:	20	56
	5679.9	2.47	- 0.13								29:	21		30:	30
	5648.6	2.49	+ 0.10								16:	21	13:		61
	5490.8	0.05	- 2.93										78:		118:
	5490.2	1.46	- 0.60										30:		86:
TiII	6559.6	2.05	- 2.14			44	59	38			58				78:
	5492.9	1.57	- 2.63			31:							31:		55
VI	6357.3	1.85	- 0.81	2.0		15:									
	6150.1	0.30	- 1.75	2.0		28	39				14:	26		38:	148
	6135.4	1.05	- 0.82	2.0		23	28	42:			14	34	44	26	98
	6119.5	1.06	- 0.48	2.0		36	32	38			12	46	45	54	126
	6090.2	1.08	- 0.13	2.0			51				12	68	34	46	122
	6081.4	1.05	- 0.58	2.0		21:	52	35			30	22	26	51	96
	6058.2	1.04	- 1.27	2.0							9	18	25:	42	48
	6039.7	1.06	- 0.59	2.0							13	24	18	64	87
	5743.4	1.08	- 1.14	2.0							12	38	13:	25	102
	5737.1	1.06	- 0.85	2.0							18	32	28	31	116
	5731.2	1.06	- 0.85	2.0		27:					25	17	38	50	131
	5727.7	1.05	- 0.99	2.0		49:									
	5727.1	1.08	- 0.26	2.0							36	79	78	96	172
	5703.6	1.05	- 0.25	2.0		25:					12	21:	20:	84	134
	5670.8	1.08	- 0.69	2.0							22	38	47:	73	110
	5668.4	1.08	- 1.13	2.0							11			28	63
	5646.1	1.05	- 1.28	2.0							21:				70
	5632.5	0.07	- 3.07	2.0							12:				30
	5627.7	1.08	- 0.57	2.0		30:					16:	17	35:		93
	5626.0	1.04	- 1.46	2.0									19:		85
	5605.0	1.04	- 1.36	2.0									11:		44
CrI	6362.9	0.94	- 2.66			29:	48:	33				18:		52:	56:
	6330.1	0.94	- 2.76			39	51				23:	22	54:	58	133:
	5783.9	3.32	- 0.18			44:					13:	20	24	13	38

TABLE 3—*Continued*

	Line	EP	log gf	V_t (hfs)	log C_6	M22 II-31	M22 IV-20	M22 IV-59	ω Cen 213	ω Cen 58	ω Cen 102	ω Cen 253	ω Cen 219
MnI	6021.8	3.07	+ 0.16	3.5		43	57	38	25	44	62	93	100
	6016.6	3.07	+ 0.00	5.4		50	44	14	19	39	36	72	89
	6013.5	3.07	- 0.15	3.8		46	48	36	27	28	26	41	88
	5516.8	2.18	- 1.44	8.9		54:					53:		77
FeI	6574.3	0.99	- 5.09			48	81	36:		92			115:
	6569.2	4.73	- 0.39			34	37	40					
	6551.7	0.99	- 5.58					30:					83:
	6481.9	2.28	- 3.00			92	131	86		94			140:
	6475.6	2.56	- 2.81			47	84	54		68			113:
	6430.9	2.18	- 2.23			171	122	106		142			164:
	6421.4	2.28	- 2.50			126	149	145		224			156:
	6420.0	4.73	- 0.17			52	63	40		63			70:
	6411.7	3.65	- 0.37			101	114	98		97			136:
	6408.0	3.69	- 1.20			98	105	70		89			126:
	6393.6	2.43	- 1.78			144	147	121		165			192:
	6358.7	0.86	- 4.09			116	88	102		59			118:
	6355.0	2.84	- 2.42			84:	78	58		68			112:
	6353.8	0.91	- 6.41			20	24:						28:
	6336.8	3.69	- 0.45			92	100	80		89			101:
	6322.7	2.59	- 2.45			88	76	80		111			114:
	6302.5	3.69	- 1.13			24:	73	69		46			61:
	6301.5	3.65	- 0.38			90	61	90		98			99:
	6173.3	2.22	- 3.26			86	66	43	43	133	112	87	99:
	6165.3	4.14	- 1.68						15	21	17:		43:
	6157.7	4.07	- 1.45			38	46	27	44	52	29:	58:	68:
	6151.6	2.18	- 3.45			50	65	49		46	65	70	112
	6082.8	2.22	- 3.55			37:	42	48	22	57	48	45	82
	6078.5	4.79	+ 0.14			38:	45:	32:	28	18	34	51	44
	6065.5	2.61	- 1.58			96	138	136	120	156	182	170	171
	6056.0	4.73	- 0.28				44	53:	36	61	36	40	66
	6027.1	4.07	- 1.16						23	33	34	50	97
	6024.1	4.55	+ 0.38			54	66	37	45	53	60	73	114
	6008.6	3.88	- 0.81			72	90	81	31	76	86	70	87
	6008.0	4.65	- 0.63			19	56:			26	13	24	38
	5987.0	4.79	- 0.32			45	40	41	19	57	18	52	54
	5976.8	3.94	- 1.23			56	45	76:	30	49	40	66	92
	5956.7	0.86	- 4.44			96	84	87	72	126	143	119	147
	5910.0	3.21	- 2.64			30	23		23	33	24	36	60
	5883.8	3.96	- 0.57			42	55	50					
	5862.3	4.55	- 0.15			67	65	49	44	56	31	62	88
	5859.6	4.55	- 0.45			57	64	47	38	63	30	44	72
	5816.4	4.55	- 0.59				56		12	62	29	64	74
	5809.2	3.88	- 1.58				46		28	42	18	40	68
	5806.7	4.61	- 0.83						24	54	36	27	48
	5778.5	2.59	- 3.60			29:			10	30	33	49	48
	5775.1	4.22	- 1.28			60:			16	38	26	47	72
	5763.0	4.21	- 0.20			77:			50	70	70	98	116
	5753.1	4.26	- 0.60			33:			40	54	48	63	90
	5701.5	2.56	- 2.13			108:			91	76	93:	127	146
	5679.0	4.65	- 0.63						30	37	26:	30	60
	5641.4	4.26	- 0.90			48:			33:	29:	24:		69
	5638.3	4.22	- 0.71			41:			41:	55:	51:		62
	5634.0	4.99	- 0.09		-33.9	23:			19:	35	15:		44

	Line	EP	log gf	V_t (hfs)	log C_6	M22 II-31	M22 IV-20	M22 IV-59	ω Cen 213	ω Cen 58	ω Cen 102	ω Cen 253	ω Cen 219
FeI (contd)	5618.6	4.21	- 1.40			18:			24:	26:	17:		51
	5586.8	3.37	- 0.42		-30.6	158:			121:	99	147:		166
	5576.1	3.43	- 0.73						82:	95	142:		130
	5569.6	3.42	- 0.69		- 30.6	122:			113:	152	169:		139
	5567.4	2.61	- 2.66			44:			48:	99			89
	5554.9	4.55	- 0.10			23:			55:	54	28:		64
	5501.5	0.96	- 3.17			242:					239:		242
	5497.5	1.01	- 3.03			235:					247:		296
CoI	5647.2	2.28	- 1.06						16:	41:			32
	5590.8	2.04	- 1.33	7.6							12:		33
	5530.8	1.71	- 1.60	2.5		18:					26:		52
NiI	6482.8	1.93	- 2.54			42	78	79		65			94:
	6327.6	1.68	- 2.82			50	54	59		66			114:
	6175.4	4.09	- 0.43				31:	33	38:	42:	31	44	29:
	6129.0	1.68	- 3.13			26	46	39	36	34	40	41	68
	6108.1	1.68	- 2.37			73	76	72	61	100	116	115	146
	6007.3	1.68	- 3.15			30	47:	49	9	39	43	25	100
	5892.8	1.99	- 1.86						53	107	96	94	126
	5847.0	1.68	- 3.17			30	42:	34	21	48	29	52	66
	5805.2	4.17	- 0.29						26		22		55
	5754.7	1.93	- 1.77			81:			58	117	102	119	141
	5748.4	1.68	- 2.98						39	82	39	41	110
	5593.8	3.90	- 0.46			23:			12:	34:	30:		37
	5592.3	1.95	- 2.21			42:			63:	70	86:		130
	5587.9	1.93	- 2.27			62:			67:	34	76:		110
	5578.7	1.68	- 2.46			78:			54:	79	130:		128
CuI	5782.1	1.64	- 1.78	2.0		60:	77:		31	73	35	63	121
ZrI	6143.2	0.07	- 1.68	2.0		15:	15:			24	24	20:	118
	6140.5	0.52	- 1.88	2.0			35:	30:		28		22:	42
	6134.6	0.00	- 1.88	2.0		10:		29		13		30:	106
	6127.5	0.15	- 1.40	2.0		27				28		23	130
	6032.6	1.48	- 0.98	2.0									30:
	5955.4	0.00	- 2.33	2.0		18:	29:			13:		15	70
	5735.7	0.00	- 2.24	2.0		12:					20		88
	5680.9	0.54	- 1.70	2.0						35			22
	5664.5	0.63	- 1.50	2.0						8:		30:	53
MoI	6030.7	1.53	- 0.71	2.0						≤15	32	17	44
	5751.4	1.42	- 1.10	2.0							14	13	23
	5570.4	1.33	- 0.56	2.0						≤10	21:		70
BaII	6496.9	0.60	- 0.10			175	197	150	119	138	170	219	226
	6147.7	0.70	+ 0.21			155	206	153	138	184	169	214	266
	5853.7	0.60	- 1.00			119	140	138	120	148	134	188	202
LaII	5808.3	0.00	- 3.17	2.0			45			14:		21:	43
	5805.8	0.13	- 2.57	2.0			44:			16	≤12	70	70
NdII	5740.9	1.16	- 1.27	2.0					≤12	≤25	≤22	≤25	49

was measured by the author, the second by one of two research assistants (M. Katz or S. Wilkerson). The weighted W_λ's for each star are listed in Table 3, where values for lines with a total weight less than 50% of the maximum weight for that star are indicated by a colon. Because of the reduced widening of these spectra compared to earlier ones, the accuracy of these measurements is somwehat less than those of previous papers of this series. For $W_\lambda \leq 75$ mÅ the error is ± 15 mÅ, while for stronger features the error is $\pm 20\%$.

III. DEDUCED ABUNDANCES

The procedures and atomic line parameters used are those of Paper I as modified in Paper III. The grid of model atmospheres used was that of Cohen, Frogel, and Persson (1978) based on the ATLAS code of Kurucz (1979) including atomic line opacities. Abundances were interpolated from the closest available models using an interpolation table corresponding to an intermediate metallicity globular cluster (Table 5 of Paper I). The microturbulent velocity for each star was derived as described in Paper I from lines of Fe I and Ti I with $W_\lambda \leq 150$ mÅ, and the values are listed in the last column of Table 1. As in Paper III, all V_t values were in the final analysis forced to be 2 km s^{-1}; it was only necessary to modify the preliminary abundances for two of the eight stars.

The final abundances obtained via our analysis for eight giants in M22 or ω Cen are listed in Tables 4A and 4B. As before, averages weighted by the individual weights for each line are given for ions with six or fewer lines where the unweighted average has an rms deviation of more than 0.2 dex. The abundance for an ion with only one line is given in parentheses and is not used in the cluster averages if the line had a weight less than 50% of the maximum weight for the star. The elemental abundance in a case where lines of two ions of the same element have been observed is weighted by the number of lines of each ion observed in the star; the cluster mean abundances given in the last two columns of Table 4 are averages of [log N/N_H] [which is log $N/N_H(*) -$ log $N/N_H(\odot)$] for the giants in each cluster irrespective of the slightly different number of lines observed in the spectra of each of the member stars.

Because of the restricted wavelength coverage of these spectra, only Ti and Sc yield ionization equilibria which can be used to check our procedures. The results of Table 4 are satisfactory, with a difference between elemental abundances deduced from neutral and singly ionized lines of Ti never larger than 0.30 dex and less than 0.10 dex for three of the five stars with reliable Ti I and Ti II abundances. Sc I lines were measured only in ω Cen, where three of the four reliable cases give an ionization equilibrium better than 0.15 dex. In the one discrepant case it is possible that the 18 mÅ line ascribed to Sc I is not real.

The abundances deduced for three members M22 listed in Table 4A show no evidence of scatter whose total range is greater than the maximum (estimated to be 0.35 dex) allowed by observational and systematic errors, except for Na, Zr, and Ba. Although Na and Zr are very temperature sensitive, so are the ions Ti I, V I, and Cr I. It is not possible to raise T_{eff} enough (invoking, for example, reddening variations within the cluster) to remove the

TABLE 4A

ABUNDANCES FOR M22 GIANTS

Element	II-31	No. of Lines	IV-20	No. of Lines	IV-59	No. of Lines	Mean for Cluster	[N/N$_{Fe}$]
OI	≤-1.57	2	≤-1.49	2	≤-1.65	2	≤-1.3[a]	≤+.5
NaI	-1.84	4	-1.08	4	-1.09	3	....	....
MgI	(-1.06)	2					(-1.06)	(+.72)
SiI	-1.56	3	-1.40	2	-1.52	1	-1.49	+.29
CaI	-1.10	16	-0.95	12	-1.17	13	-1.07	+.71
ScII	-1.55	4	-1.52	1			-1.54	+.24
TiI	-1.23	14	-1.10	15	-1.17	14		
TiII	-1.24	2	-0.80	1	-1.14	1	-1.16	+.62
	-1.23		-1.08		-1.17			
VI	-1.46	9	-1.53	5	-1.52	3	-1.50	+.28
CrI	-1.60	3	-1.66	2	-1.92	1	-1.73	+.05
MnI	-1.77	4	-1.82	3	-2.06	3	-1.88	-.10
FeI	-1.80	44	-1.66	36	-1.87	32	-1.78	0.00
CoI	(-2.03)	1					(-2.03)	(-.25)
NiI	-1.84	11	-1.53	7	-1.54	7	-1.64	+.14
CuI	(-2.25)	1	(-2.18)	1			(-2.22)	(-.44)
ZrI	-1.51	5	-1.08	3	-1.03	2	-1.21	+.57
BaII	-1.72	3	-1.35	3	-1.63	3	-1.57	+.21
LaII			-0.66	2			-0.66	+1.12

[a] Mean for cluster includes 0.2 dex CO correction.

TABLE 4B

ABUNDANCES FOR ω CENTAURI GIANTS

Star	213	No.of	58	No.of	102	No.of	253	No.of	219	No.of
R(V-K)	0.06	Lines	0.13	Lines	0.16	Lines	0.25	Lines	0.42	Lines
OI	≤-1.76	1	-1.93	2	-1.67	1	≤-1.64	1	-1.23	2
COcorr.	0.2		0.3		0.3		0.3		0.3	
NaI	-1.75	4	1.27	6	-1.35	5	-0.83	6	-1.28	6
MgI	-1.82	1	-1.53	1	-1.65	2	-1.90	1	-0.83	2
AlI	...		...		...		-0.15	2	-0.68	2
SiI	-1.60	2	-2.05	2	-1.87	2	-1.21	3	-1.08	3
CaI	-1.28	12	-1.09	17	-1.26	12	-0.66	8	-0.74	15
ScI	-1.19	1	-1.68	1	(-1.25)	1	-0.79	1	-1.22	1
ScII	-1.82	2	-1.57	2	-1.76	3	-0.70	1	-1.27	3
	-1.61		-1.61				-0.75		-1.26	
TiI	-1.03	21	-1.27	18	-1.37	21	-1.08	19	-0.83	23
TiII	...		-1.06	1	(-1.56)	1	...		-0.89	2
			-1.26						-0.83	
VI	-1.40	17	-1.70	14	-1.60	15	-1.33	14	-1.20	19
CrI	-1.98	2	-1.96	3	-1.34	2	-1.63	3	-1.36	3
MnI	-1.95	3	-2.09	3	-1.94	4	-1.71	3	-1.85	4
FeI	-1.79	34	-1.82	47	-1.89	33	-1.58	25	-1.55	48
CoI	(-1.55)	1	(-1.51)	1	-2.17	2	...		-1.85	1
NiI	-1.60	13	-1.69	14	-1.72	13	-1.52	8	-1.23	15
CuI	-2.31	1	-2.32	1	-2.66	1	-2.30	1	-1.86	1
ZrI	...		-1.40	7	-1.52	2	-1.23	6	-1.08	9
MoI	...		≤-1.72	2	-1.14	3	-1.09	2	-1.11	3
BaII	-2.09	3	-2.07	3	-2.00	3	-1.11	3	-1.05	3
LaII	...		-1.73	2	≤-1.96	1	-0.83	2	-0.82	2
NdII	≤-1.29	1	≤-1.27	1	≤-1.18	1	≤-0.82	1	-0.57	1

range in Na I, without introducing problems in these other ions. Also the interstellar line data presented in the appendix suggest that M22 II-31 is less reddened than the other two giants, so its $T_{\rm eff}$ should perhaps be lowered, which will make the Na discrepancy worse. The scatter in Zr can be dismissed, as all Zr I lines are very weak, and some could be noise rather than real features. However, the Ba and especially the Na range are so large that they must be real. We note that in the case of all three elements, star II-31 has lower abundances than the other M22 giants. We will return to this point after discussing the pattern of abundances seen in the ω Cen giants.

The mean [Fe/H] for M22 from this high dispersion analysis is -1.78 dex. This is close to that determined by Zinn (1980), namely -1.86, via integrated light photometry, as would be expected for photometry calibrated using the results of earlier papers in this series. Peterson (1980*a*) has presented a preliminary analysis of four stars in M22, and finds a range in [Fe/H] of 0.6 dex. However, the $T_{\rm eff}$ she used are from Fe I excitation, and disagree substantially with those derived from $V-K$ colors. The difference between her $T_{\rm eff}$ values and those of Cohen and Frogel vary between 150 K and 400 K; this may give rise to the scatter in iron abundance she sees.

IV. VARIATION OF THE ELEMENTS WITHIN ω CENTAURI

The five giants analyzed in ω Cen are, as shown in Table 4B, clearly different in their chemical compositions. We divide the stars into a group of metal-poor (denoted MP giants) (including ROA 213, 58, and 102) and metal-rich (denoted MR) ones (ROA 253 and 219) based on their $R(V-K)$ values, which depend only on their location in a theoretical H-R diagram. Although there most likely is a continuous progression of abundances from metal-poor to metal-rich in ω Cen, we adopt this simplification of two discrete groups to improve the statistics in the subsequent discussion. Average abundances for the MP and MR groups for each element are listed in Table 5, as are the difference between them.

First, we note that all elements with reliable abundances are enhanced in the MR giants of ω Cen. However, the degree of enrichment from the MP to MR group is not uniform. The light elements Na, Mg, Si, Ca, and Sc are significantly enhanced in the MR group, averaging 0.5 dex higher or a factor of 3. The Fe peak elements from Ti to Ni are enhanced by a smaller factor of about 1.8. The

TABLE 5

ABUNDANCES FOR METAL-POOR AND METAL-RICH ω CENTAURI GIANTS

$\langle R(V-K)\rangle$ Element	ROA 213,58,102 $[N/N_{\rm H}]$ 0.12	ROA 253,219 $[N/N_{\rm H}]$ 0.33	$\Delta[N/N_{\rm H}]$
O	≤1.50	≤1.15	...
Na	−1.46	−1.06	+0.40
Mg	−1.67	−1.37	+0.30
Al	...	−0.42	...
Si	−1.84	−1.15	+0.69
Ca	−1.19	−0.70	+0.49
Sc	−1.66	−1.01	+0.65
Ti	−1.22	−0.96	+0.26
V	−1.57	−1.37	+0.20
Cr	−1.76	−1.50	+0.26
Mn	−1.99	−1.78	+0.21
Fe	−1.83	−1.57	+0.26
Co	(−1.85)	−1.85	(0.0)
Ni	−1.67	−1.38	+0.29
Cu	−2.43	−2.08	+0.35
Zr	−1.46	−1.16	+0.30
Mo	(−1.45)	−1.10	(+0.35)
Ba	−2.05	−1.08	+0.97
La	(−1.87)	−0.83	(+1.04)
Nd	≤−1.25	≤−0.70	...

data for the heavier elements is of lower quality, but Ba and probably the rare earths are enhanced by a factor of 10.

We now consider separately the two stars in the MR group. The progression of metallicity as inferred from $R(V-K)$ in the MP giants, then ROA 253, with ROA 219 being the most metal-rich. This progression is violated for the elements Na, Mg, Al, Ca, Sc, Mn, and Mo. Errors of less than 0.1 dex in abundances in both ROA 253 and ROA 219, which are quite likely, will remove the discrepancy in Ca, Mn, and Mo. This leaves Na, Mg, Al, and Sc as reliably more abundant in ROA 253 than in ROA 219, with most other elements studied here more abundant in the latter.

These stars have luminosities ranging from $M_{\rm bol} = -2.2$ to -3.1 mag, well below that of the red giant tip. The two most metal-rich stars ROA 253 and 219 have bolometric magnitudes -2.2 and -2.7 mag, respectively. It therefore is impossible to ascribe the pervasive abundance variations seen among the ω Cen giants studied here to mixing of nuclear processed materials from the stellar interior to the photosphere. Such mixing is believed to take place only in phase of stellar evolution following the He flash at $M_{\rm bol} \approx -3.4$ (see, for example, Iben 1974) and to involve only the lighter elements such as C and N, most certainly not those of the Fe peak, which cannot be produced even in the core until much later evolutionary phases. As we are here not considering C or N, we therefore do not consider mixing processes to have affected the abundances of the ω Cen giants.

At this point, a brief review of the predictions of theoretical nucleosynthesis calculations seems required. Supermassive objects, whose nucleosynthesis has been discussed by Wagoner (1968), do not produce enough heavy elements to be responsible for the abundance range in ω Cen. Furthermore, one such explosion would completely disrupt the protoglobular cluster, making it difficult to produce the violation of progression discussed for Na, Mg, Al, and Sc above. Also the ratio [Al/Mg] is always $+0.2$ dex in Wagoner's calculations, which is quite different from that observed in ROA 253. The products of such supermassive explosions do not seem relevant to the present case.

As outlined by Arnett (1971), explosive carbon burning in massive stars (1–20 $M_\odot$) is believed to have produced most of the presently observed Ne, Na, Mg, Al and Si; explosive oxygen burning (presumably in a different zone of the same massive star or later during the explosion) then produces S, Cl, Ar, and Ca, while explosive Si burning produces the Fe peak nuclei from Ti through Ni. The neutron excess, η, controls the odd/even ratio of elements produced by explosive carbon burning, particularly the Na/Mg and Al/Mg ratios. Arnett (1971) states that $\eta \approx 0.1Z$, where Z is the total abundance by number of heavy elements with respect to hydrogen, so that for solar metallicity, $\eta \approx 2 \times 10^{-3}$. He therefore expects that in metal-poor stars, η will be significantly lower than in metal-rich stars. If hydrostatic C burning, as well as H and He burning, has been completed in a massive metal-poor star prior to the explosion, then larger values of η up to 5×10^{-3} can be reached (Arnett 1973). A minimum core mass of 4 $M_\odot$ is required for hydrostatic C burning, which corresponds to a total mass (ignoring mass loss) of 12 $M_\odot$ using the transformation of Arnett (1978). Pardo, Couch, and Arnett (1974) give detailed calculations of various abundance ratios as functions of η, and discuss the effects of varying initial C/O ratios. They find that decreasing C/O for fixed heavy element metallicity is equivalent to increasing η.

There are thus two specific tests of this scenario. Simplifying greatly, the first is whether the Al/Mg–Ng/Mg correlation in various stars behaves as predicted for η as the only variable. The second is whether η behaves as though it is proportional to metallicity, or equivalently whether the metallicity of the exploding object is related to the metallicity of the star to be formed out of its ejecta (which in turn puts constraints on the dilution of the ejecta). Peterson (1980*b*), in her study of moderately and strongly metal-poor field stars, finds that both tests are satisfied, while Spite and Spite (1980) do not find the predicted large Al overdeficiencies in very metal poor cool giants.

Figure 1 shows the correlation of [Na/Mg] with [Al/Mg] for field stars from Peterson (1980*b*), a compilation of older data by Arnett (1971), and our results for ROA 219 and 253 in ω Cen. The theoretical relationship as a function of η is indicated using the calculations of Pardo, Couch, and Arnett (1974). It is apparent that the theory fails to reproduce the observed pattern for large values of η, though it does so for $\eta < 2 \times 10^{-3}$. Furthermore, ROA 253 in ω Cen, an old metal-poor giant, has the largest value of η yet found, while ROA 219, a member of the same cluster, and of similar [Fe/H], has a much smaller value of η ($\approx 5 \times 10^{-4}$), although still higher than would be expected for its [Fe/H]. To have produced such large neutron excesses, the massive star(s) which exploded must therefore have undergone hydrostatic carbon burning prior to their death, implying a minimum mass of 12 $M_\odot$. Even so, it is difficult to contrive such large values of η in metal-poor stars in the context of the present theoretical framework.[3]

What are the implications of these large neutron excesses? Howard *et al.* (1972) have explored the isotopes produced by seed nuclei reacting with the free protons, neutrons, and α-particles liberated in the explosive C burning shell. Among the elements believed to be produced in this fashion is scandium. Production of some isotopes of the heavy elements beyond the Fe peak is discussed in connection with the problem of the Allende meteorite anomalies by Lee *et al.* (1979). Ba, Nd, and other rare earths can be synthesized under such conditions. It is therefore extremely interesting that ROA 253, which has the largest value of η, also has the highest scandium abundance of the five ω Cen stars studied and strongly enhanced Ba and Nd.

[3] Large values of η ($\approx 10^{-2}$) also occur when C is ignited in the degenerate cores of intermediate mass stars (4–8 $M_\odot$), but elements heavier than Mg are not produced due to the low temperatures (see Couch and Arnett [1975] for details). Thus this situation of high η is not relevant for the ω Cen stars.

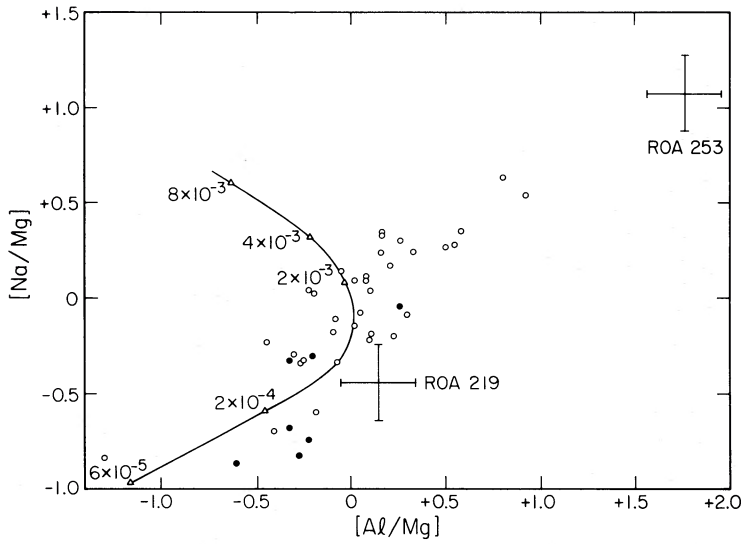

FIG. 1.—The [Na/Mg] and [Al/Mg] ratios are shown for metal-poor field stars with data from Peterson (1980*b*), indicated by the solid circles, and for field stars from a compilation of older data by Arnett (1971), indicated by the open circles. The positions of the ω Cen giants ROA 219 and 253 are marked by crosses. The size of each cross is typical of the observational and systematic errors afflicting all of the data displayed. The theoretical relationship from calculations of explosive nucleosynthesis by Pardo, Couch, and Arnett (1974) is indicated as a function of the neutron excess by the smooth curve. Values of the neutron excess are given at positions along this curve marked by open triangles.

A plausible scenario for the chemical history of ω Cen then requires that several massive stars became supernovae in the protoglobular cluster prior to the formation of the low mass stars we see today. Explosive carbon and oxygen burning occurred preferentially in these supernovae with respect to explosive silicon burning, and the neutron excess, η, was large and variable, reaching values up to $\eta \approx 10^{-2}$. The resulting large flux of secondary neutrons induced additional reactions which in turn produced large enhancements of scandium and of the heavy elements beyond the Fe peak.

Two ways can be imagined to produce the range of metallicity seen in ω Cen: successive episodes of supernova explosions, each contaminating most of the protoglobular cluster gas, and each followed by star formation, versus approximately simultaneous supernovae, the ejecta of which had differing chemical compositions and/or differing dilutions with primordial gas, followed by a single burst of star formation. In this context it is interesting to note that ω Cen is the most luminous (and probably the most massive) globular cluster in the Galaxy. Thus it might be best able to retain gas and survive intact after repeated supernova explosions. At a fixed metallicity, an age spread of more than 3×10^9 years would be enough to create an observable dispersion of the giant branch in $V-K$; hence, it would show up as a lack of correlation between $R(V-K)$, the metallicity parameter based on location in the H-R diagram, and the spectroscopically determined abundances of giants in ω Cen. Although five stars is inadequate for such a test, the results so far are encouraging, as shown in Table 6, where [Fe/H] is predicted from the $R(V-K)$ values using straight line segments to fit the three known points [−2.3 for M92 with $R(V-K) = 0.0$, −1.7 for M3 and M13, with $R(V-K) = 0.2$, and −1.3 for M71, with $R(V-K) = 0.7$]. This test should be extended to more stars and particularly to those with large values of $R(V-K)$. However, since massive progenitor stars which have very short evolutionary lifetimes are suggested by the high values of η, the age spread within the ω Cen giants we see today may be too small to be detectable.

We assume that most halo stars are not escapees from globular clusters, but rather they are formed under less dense conditions than existed in the protoglobular clusters. We then suggest that the supernovae which produced the metals seen in field stars to have been of lower mean mass, so as not to have undergone hydrostatic carbon burning prior to explosion. Thus the correlation between metallicity and η predicted by Arnett (1971) was preserved, as has been found by Peterson (1980*b*) from analysis of metal poor field stars. Metal-poor halo field stars also show Ba overdeficiencies with respect to Fe, as would be expected for small neutron excesses, unlike the globular cluster stars.

TABLE 6

COMPARISON OF SPECTROSCOPIC AND EMPIRICAL (giant branch locations) METALLICITIES

Star (ROA)	[Fe/H] Spectra	[Fe/H] $R(V-K)$
213	−1.8	−2.1
58	−1.8	−1.9
102	−1.9	−1.8
253	−1.6	−1.65
219	−1.55	−1.5

The spread in Na abundance seen in M22 here and by Peterson (1980*c*) in M13 must be related to the phenomena seen in ω Cen and yet somehow involve supernovae in which only explosive C burning, but not O or Si burning, occurred. It is also interesting to note that strong enhancements of Ba and the rare earths are common in globular cluster giants (see Paper III), implying that large neutron excesses also were frequent among the supernovae which occurred in the protoglobular clusters.

V. SUMMARY

A detailed abundance analysis has been performed using high dispersion echelle spectra for three members of M22 and five giants in ω Cen. The three stars in M22 are chemically identical, except for sodium, and less definitely, for barium. There is a range of 0.8 dex in the derived Na abundance of these stars, far larger than that allowed by the errors.

The ω Cen giants show that a range of chemical composition exists for all elements in this unique cluster. However, as one compares metal-poor with metal-rich stars in ω Cen, each element is not enhanced by a constant factor. In the more metal-rich ω Cen giants studied here, the light elements Na, Mg, Al, Si, Ca and Sc are all enhanced by a factor of about 3, while the Fe peak elements are enhanced by only a factor of 1.8. Barium and the rare earths are enhanced by a factor of 10. Furthermore, the two most metal-rich ω Cen stars studied have vastly different Na, Mg, Al, and Sc abundances, while most other elements are of comparable abundance. Large neutron excesses (implying supernova progenitors with $M > 12\ M_\odot$) are required if the observed enhancement of the light elements is to be produced via explosive carbon and oxygen burning in supernovae. Reactions involving neutrons will then occur during the supernova event, which presumably produce the strong enhancement of Ba and the rare earths seen in the metal-rich ω Cen stars. Such large neutron fluxes are not expected in low mass metal-poor supernovae, and the data of Peterson (1980*b*) support low neutron excesses for metal-poor field stars. This indicates that the supernovae in protoglobular clusters were in the mean more massive than those in the galactic disk in the solar neighborhood.

APPENDIX

We present in Table 7 some data on the radial velocities, interstellar lines, and presence of emission in the wings of Hα for the program stars in M22 and ω Cen. The radial velocities were determined from the 5577 Å night sky line only, as no comparison spectra were used due to the small order spacing. The radial velocities are accurate to ± 5 km s^{-1} and indicate that all the stars are members of M22 or ω Cen. Most of the spectra show evidence for emission in the red (R), blue (B), or both (R + B) wings of Hα, with uncertain cases indicated appropriately in the last column of the table. In Paper III, none of the giants in metal-rich clusters had emission in the wings of Hα. If such emission is, as suggested by Cohen (1976), indicative of mass loss and the presence of extensive circumstellar material, the initial evidence of this series of papers is that the mass loss rate is in the mean higher in metal poor clusters than in the metal rich ones. This tentative indication of a mass loss rate increasing as Z decreases is in the same sense as that hesistantly suggested by Frogel, Persson, and Cohen (1980) from their study of a large number of globular clusters on the basis of the slopes of the upper giant branches as compared to those of the lower giant branches in the H-R diagram. Theoretical reasons (e.g., Rood 1973) can be advanced for a mass loss rate whose dependency on metallicity is of the opposite sign to that required by the observational evidence, but perhaps this should be taken as an indication that our understanding of mass loss mechanisms and their dependence on metallicity is still incomplete. Speculating still further, it should be recalled that the metallicity assigned to the standard "metal rich" globular clusters is now considerably below the solar value, as described in Paper III. If the suggested decrease in mass loss rate should persist as metallicities increase beyond that of M71, it is possible that in old systems with solar metallicity, the upper AGB can be populated to a level significantly above

TABLE 7

V_r AND INTERSTELLAR Na COMPONENTS

		Interstellar Component				Interstellar Component		
Star	V_r (km s^{-1})	W_λ (mÅ) (5889)	W_λ (mÅ) (5895)	V_r (km s^{-1})	W_λ (mÅ) (5889)	W_λ (mÅ) (5895)	V_r (km s^{-1})	Hα Emission
M22:								
II-31	−156	115:	...	+32	360	280	−6	R?
IV-20	−163	335:	...	+32	455:	370:	0	R + B
IV-59	−160	230:	215:	+23	405:	375:	−12	B?
ω Cen:								
213	+229	320	205	−11	...	...	...	No?
58	+239	325	255	−10	...	...	...	R + B
102	+247	410	380	−3	...	...	...	R
253	+231	230	155	−3	...	...	...	R + B?
219	+237	415	300	−6	...	...	...	R? + B?

the first red giant tip. This suggestion would have important ramifications for the interpretation of integrated light photometry of composite stellar systems and more work in this area seems urgent.

The M22 stars show two interstellar components, both of which are fairly strong, as would be expected from the low galactic latitude of the cluster. The component at $+30$ km s^{-1} appears to vary greatly in column density over the cluster; it is strong in the two giants in the SE sector and much weaker in the NW sector star. The column density of Na I from the component at -6 km s^{-1} is approximately constant at 1×10^{13} atoms cm^{-2}. Using the constants of Cohen (1975) for less dense interstellar clouds in the galactic plane and the ratio $N_H/E(B-V)$ of Jenkins and Savage (1974), we find $E(B-V) = 0.42^{+0.25}_{-0.15}$ mag, for this component alone. Our adopted reddening, based on Harris and Racine's (1979) compilation and Zinn's (1980) integrated light photometry, is 0.36 mag, close to that expected. The second interstellar component will give rise to substantial reddening in at least the SE quadrant of the cluster. Such variations in the interstellar line components imply that reddening variations alone can induce a spurious scatter in the width of the giant branch in an H-R diagram.

The ω Cen giants show a single strong interstellar component at V_r close to 0 km s^{-1}. This cloud also appears to vary in column density over the cluster, with a mean N(Na I) of 4×10^{12} atoms cm^{-2}. With the constants described above, this yields $E(B-V) = 0.17^{+0.10}_{-0.05}$ mag, agreeing well with the 0.11 mag found by Cannon and Stobie (1973) and adopted by PFCAM.

REFERENCES

Arnett, W. D. 1971, *Ap. J.*, **166**, 153.
———. 1973, *Ap. J.*, **179**, 249.
———. 1978, *Ap. J.*, **219**, 1008.
Butler, D., Dickens, R. J., and Epps, E. 1978, *Ap. J.*, **225**, 148.
Cannon, R. D., and Stobie, R. S. 1973, *M.N.R.A.S.*, **162**, 207.
Cohen, J. G. 1975, *Ap. J.*, **197**, 117.
———. 1976, *Ap. J.* (*Letters*), **203**, L127.
———. 1978*a*, *Ap. J.*, **223**, 487 (Paper I).
———. 1978*b*, NATO Advanced Study Institute on Globular Clusters (to be published).
———. 1979, *Ap. J.*, **231**, 751.
———. 1980*a*, *Ap. J.*, **241**, 981 (Paper III).
———. 1980*b*, in *Star Clusters*, ed. J. Hesser (Dordrecht: Reidel), p. 385.
Cohen, J. G., Frogel, J. A., and Persson, S. E. 1978, *Ap. J.*, **222**, 165.
Couch, R. G., and Arnett, W. D. 1975, *Ap. J.*, **196**, 791.
Dickens, R. J., and Woolley, R. 1967, *Roy. Obs. Bull.*, No. 128.
Eggen, O. J. 1977, *Ap. J.*, **213**, 767.
Frogel, J. A., Persson, S. E., and Cohen, J. G. 1980, *Ap. J.*, in press.
Harris, W. E., and Racine, R. 1979, *Ann. Rev. Astr. Ap.*, **17**, 241.
Hesser, J. E. 1976, *Pub. ASP*, **88**, 849.
Hesser, J. E., and Harris, G. L. H. 1979 *Ap. J.*, **234**, 513.
Hesser, J. E., Hartwick, F. D. A., and McClure, R. D. 1977, *Ap. J. Suppl.*, **33**, 471.
Howard, W. M., Arnett, W. D., Clayton, D. D., and Woosley, S. E. 1972, *Ap. J.*, **175**, 201.
Iben, I., Jr. 1974, *Ann. Rev. Astr. Ap.*, **12**, 215.
Jenkins, E. B., and Savage, B. D. 1974, *Ap. J.*, **187**, 243.
Kurucz, R. L. 1979, *Ap. J. Suppl.*, **40**, 1.
Lee, T., Schramm, D. N., Wefel, J. P., and Blake, J. B. 1979, *Ap. J.*, **232**, 854.
Lloyd Evans, T. 1975, *M.N.R.A.S.*, **171**, 647.
———. 1978, *M.N.R.A.S.*, **182**, 293.
Norris, J. 1978, NATO Advanced Study Institute on Globular Clusters (to be published).
Pardo, R. C., Couch R. G., and Arnett, W. D. 1974, *Ap. J.*, **191**, 711.
Persson, S. E., Frogel, J. A., Cohen, J. G., Aaronson, M., and Matthews, K. 1980, *Ap. J.*, **235**, 452 (PFCAM).
Peterson, R., 1980*a*, in *Star Clusters*, ed. J. E. Hesser (Dordrecht: Reidel) p. 461.
———. 1980*b*, *Ap. J.*, **235**, 491.
———. 1980*c*, *Ap. J.* (*Letters*), **237**, L87.
Rood, R. T. 1973, *Ap. J.*, **184**, 815.
Searle, L., and Zinn, R. 1978, *Ap. J.*, **225**, 357.
Spite, M., and Spite, F. 1980, *Astr. Ap.*, **89**, 118.
Wagoner, R. V. 1968, *Ap. J. Suppl.*, **18**, 247.
Woolley R. v.d. R., *et al.* 1966, *Roy. Obs. Ann.*, No. 2.
Zinn, R. 1980, *Ap. J. Suppl.*, **42**, 19.

JUDITH G. COHEN: Department of Astronomy 105-24, California Institute of Technology, Pasadena, CA 91125.